GRADIVA

Volume 65 | Issue 02 | February 2026
DOI: 10.5281/zenodo.18720371

A Fuzzy Logic Based Evaluation of Electric Vehicle Battery State of Charge and State of Health in a Regenerative Braking State

Crescent Onyebuchi Omeje[1]* & Chizindu Stanley Esobinenwu[2]

1,2.Department of Electrical/Electronic Engineering, University of Port Harcourt,
East-West Road Choba, PMB 5323, Rivers State Nigeria.
Email: [1]crescent.omeje@uniport.edu.ng (*Corresponding Author), [2]chizindu.esobinenwu@uniport.edu.ng

Abstract

This paper focused on developing a fuzzy logic-based control system that dynamically regulated energy recovery during regenerative braking. An optimal charging condition with minimized battery degradation during acceleration and braking processes were illustrated. The proposed model employed three key inputs that involved braking force, motor speed, and state of charge of lithium-ion battery with an output that depicted the charging and discharging current. Fuzzy Logic Controller demonstrated superior adaptability and robustness in handling dynamic braking situations for energy recovery enhancement and battery longevity. Using triangular, trapezoidal and Gaussian membership functions within a Mamdani inference system and centroid defuzzification, fuzzy surfaces were generated to estimate SOH degradation and drift in SOC. Simulation results showed that SOH degradation ranged from 0.30 to 0.85 pu, with a mean value of 0.489 pu and a standard deviation of ±0.221 pu. The steepest degradation occurred at 20% SOC with Capacity rate of four (4C) under a highway braking process. Conversely, At 80% SOC, the state of health degradation remained lowest while maintaining 0.44 pu for highway drive, 0.39 pu for suburban and 0.31 pu for city drive conditions. Appreciable thermal acceleration was achieved after 450 C. A drift error of 0.86 p.u was realized under frequent braking.

Keywords: *Discharge Rate, Electric Vehicle, Fuzzy Logic Controller, Lithium-Ion Battery, Regenerative Braking, State of Charge (SOC) and State of Health (SOH).*

1. INTRODUCTION

The harmful effects of fossil fuel gas emissions to human health and the consequential impacts on the ozone-layer depletion have led to the evolution of electric vehicles. The applications of renewable energy as a source of power supply and battery back-up in automobile drives are gaining momentum. This process can significantly enhance the battery's efficiency and lifespan thereby contributing to the overall sustainability of electric vehicles [6]. Energy recovery and its optimization in most electric vehicles are very expedient. To ensure continuity and also to avert dissipation during braking, some techniques have been adopted for energy recovery optimization and battery state of health in Electric Vehicle drive as reported in [1] – [5]. The state of charge and state of health forms the major determinant of the battery operational efficiency and electric vehicle mileage. Lithium-ion batteries of high energy density and efficiency are commonly applied in Electric Vehicles. In [6] – [7], optimizing the battery state of charge and state of health in regenerative braking state reduces its fading and thermal run-away. In this paper, a fuzzy logic based state of charge and state of health evaluation was considered under regenerative braking states. In addition, a multi-dimensional assessment of the battery state of charge and state of health at varied capacity rate (C) and temperature drift under regenerative braking was presented.

Volume 65 | Issue 02 | February 2026
DOI: 10.5281/zenodo.18720371

2. RELATED LITERATURE

Energy loss due to friction in the axles and wheel of electric vehicle during braking can be regenerated to charge the battery pack of the electric vehicle. In [8] – [11], regenerative braking in electric vehicle drives was elaborately illustrated in terms of the braking power of the auto-electric drive with permanent magnet synchronous machine and lithium-ion state of charge at different drive topology. In [12], Lithium-ion battery was preferred to Lead-acid and nickel-metal hydride batteries for long-range drive process. In [13], it is proven that energy recovery efficiency of regenerative braking system in electric vehicles devoid of internal combustion engine reduces the risk of global warming and greenhouse gas emission.

In [14] – [16], the impact of battery management and state of charge optimization in electric vehicle as strategies for reducing carbon emission was discussed. In [17], energy management systems of electric vehicles were compared with the internal combustion engine vehicles in terms of their operating and maintenance costs as well as the simplicity in their design. In other reviewed literature and for energy management of electric vehicles, it was shown that battery state of charge and state of health depend on the temperature, rate of charge and depth of discharge [18] – [26]. It also addressed previous research gaps, particularly around temperature effects on SOC and SOH during regenerative braking.

Other studies, as referenced in [27], have improved on using power electronic converters to enhance SOC recovery during braking. Yet, even with advances in SOC optimization, SOH degradation remains a challenge, especially with frequent braking or extreme environmental conditions.

A real-time optimization algorithm capable of managing both SOC and SOH during braking events showing promise for real-world applications was presented in [28]-[29]. This present study therefore improved on the reviewed literature framework by examining fuzzy logic based SOC and SOH correlations under EV-specific stressors like regenerative braking, thermal variation and high-rate of discharge where adaptive and non-deterministic modeling are of essence..

3. METHODOLOGY

3.1 Mathematical Modeling and Data Framework for SOC and SOH

Mathematical equations were derived to describe the relationship between SOC, SOH, and the energy recovered during regenerative braking. The equations were modeled based on electrical and mechanical dynamics. The electrical equations as referenced in [21] are presented in (1)-(19) which formed the basis for the control strategy developed in this research. The battery state of charge is given by (1)

$$\mathrm{SoC(t)} = \mathrm{SoC(t-1)} + \frac{\mathrm{P_{in}(t)} - \mathrm{P_{out}(t)}}{\mathrm{C}} \qquad (1)$$

Where:

$\mathrm{SoC(t)}$: state of charge at time (t)

$\mathrm{P_{in}(W)}$: power input (charging power)at time

$\mathrm{P_{out}(W)}$: power output (discharging power)at time

C: battery capacity (AH)

Volume 65 | Issue 02 | February 2026
DOI: 10.5281/zenodo.18720371

Considering the efficiency during charging and discharging state, the power input and output can be derived as presented in (2) and (3).

When charging:

$$P_{in}^{eff}(t) = \eta_{charge} * P_{in}(t) \tag{2}$$

When discharging:

$$P_{out}^{eff}(t) = \frac{P_{in}(t)}{\eta_{discharge}} \tag{3}$$

Substituting (2) and (3) into (1) gave rise to (4)

$$SoC(t) = SoC(t-1) + \frac{\eta_{charge} * P_{in}(t) \ - \frac{P_{in}(t)}{\eta_{discharge}}}{C} \tag{4}$$

Permanent Magnet Synchronous Machines (PMSMs) are particularly well-suited for regenerative braking because of their high power density and impressive efficiency, even at low speeds. As the stator's magnetic field rotates, the rotor which is in perfect synchronism with the magnetic field locks onto it and rotates at the same synchronous speed which forms the major principles of operation of PMSM. Unlike induction motors, PMSM has no slip between its rotor and stator's field, a crucial factor that contributes to its efficiency [11]. By converting kinetic energy into electrical energy, regenerative braking helps maintain both SOC and SOH in Lithium Ion batteries, extending their lifespan and improving vehicle range. With the application of power electronic converters and integration of PMSMs, energy recovery is not only efficient but very benign.

Mathematical Models of the Permanent Magnet Synchronous Machines are presented in (5) –(10)

$$V_f = R_f i_f + L_f \frac{di_f}{dt} \tag{5}$$

$$V_a = C_1 i_f \omega + L_a \frac{di_a}{dt} + R_a i_a \tag{6}$$

$$J\frac{d\omega}{dt} = C_2 i_f i_a + C_2 \omega \tag{7}$$

Taking $x_1 = i_f, x_2 = i_a, x_3 = \omega$, voltages V_a and V_f as independent control inputs.

The system state equations representing the AC machine is given as: (8)- (10)

$$(\dot{x_1}) = -\frac{R_f}{L_f}x_1 + \frac{V_f}{L_f} \tag{8}$$

$$(\dot{x_2}) = -\frac{R_a}{L_a}x_2 - \frac{C_1}{L_a}x_1x_3 + \frac{V_a}{L_a} \tag{9}$$

$$(\dot{x_3}) = \frac{C_2}{J}x_3 + \frac{C_2}{J}x_1x_2 \tag{10}$$

Where:

V_f: field voltage; R_f: field resistance; L_f: field inductance

V_a: armature voltage

R_a: armature resistance

Volume 65 | Issue 02 | February 2026
DOI: 10.5281/zenodo.18720371

L_a: armature inductance

J: inertia

Furtherance to the above electrical equations is the mechanical dynamics of the electric vehicle equations which are derived from Figure 1 under motoring and braking mode as referenced in [30].

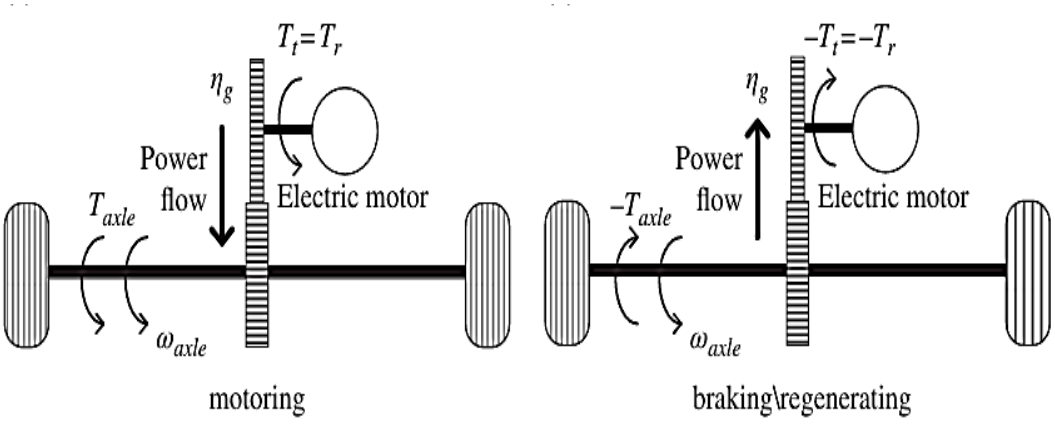

Figure 1: Mechanical dynamics of Electric Vehicle under (a) motoring and (b) regenerating modes

Total torque required at the drive axle (T_{axle}) is the sum of motive torque (T_{motive} is due to linear motion) and the torque required to overcome the inertia also known as the accelerating torque which is given by (11)

$$T_{axle} = T_{motive} + J_{axle}\frac{d\omega}{dt} = T_{motive} + J_{axle}\alpha_{axle} \quad (11)$$

$$T_{motive} = r \times [m\frac{dv}{dt} + (A + mg\sin\theta) + Bv + Cv^2] \quad (12)$$

Since vehicle linear speed is related by the angular speed and distance as shown in (13) and (14)

$$v = r \times \omega \quad (13)$$

$$\frac{v}{r} = \omega \quad (14)$$

Substituting (12) and (14) into (11) with proper rearrangement gives rise to equation (15)

$$T_{axle} = r \times \left[m\frac{dv}{dt} + (A + mg\sin\theta) + Bv + Cv^2\right] + \frac{J_{axle}}{r} \times \frac{dv}{dt} \quad (15)$$

Traction torque T_t is the torque developed on the output shaft of electric motor. Traction torque is directly geared to the drive-axle torque and both are related to efficiency of gearing as shown in (16)

$$T_{axle} = \eta_g \eta_m T_t \quad (16)$$

$$T_t = \frac{T_{axle}}{\eta_{g1}\,\eta_{g2}} = \frac{r}{\eta_{g1}\,\eta_{g2}}\; r \times \left[\left(m + \frac{J_{axle}}{r^2}\right)\frac{dv}{dt} + (A + mg\sin\theta) + Bv + Cv^2\right] \quad (17)$$

Where : A is the coefficient of the rolling resistance, B is the coefficient of the rotational losses or spinning losses. C is the coefficient of the aerodynamic drag. T_{axle} = axle torque (Nm), J_{axle} is moment of inertia (Kgm^{-2}). T_{motive} is the motive torque (Nm) due to linear

Volume 65 | Issue 02 | February 2026
DOI: 10.5281/zenodo.18720371

motion. α_{axle} is the angular acceleration rad. per sec. m is mass of the vehicle in Kg. v is the linear speed of the vehicle m/s. η_{g1} η_{g2} represents the efficiencies of gearing in motoring and regenerative braking mode.

A key component in drives is the power electronics interface, typically a bidirectional DC-DC converter that regulates energy flow between the motor and the battery, ensuring efficient regeneration. The conventional dc-dc boost converter is shown in Figure 2 while the Mathematical Model for the Boost Converter are presented in equations (18)-(21)

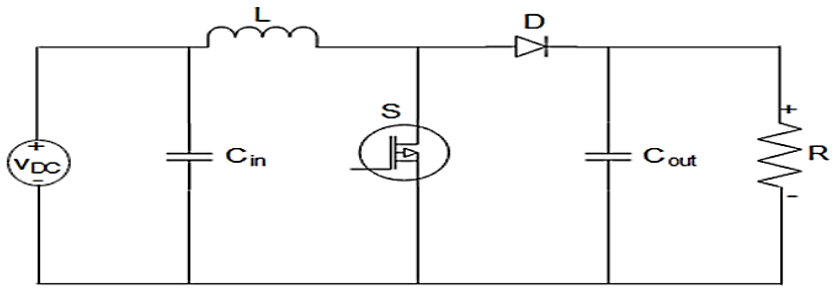

Figure 2: Equivalent Circuit of a DC- DC Boost Converter

Figure 2 shows the equivalent circuit of a DC-DC boost converter used for this study. The converter consists of 2(two) MOSFET or IGBT switches, an inductor, a capacitor, and a diode that is connected to the load circuit.

$$\text{Inductor (L)} = \frac{V_{input}\left(V_{output} - V_{input}\right)}{f_{sw} * \Delta I * V_{output}} \quad (18)$$

$$\text{Capacitor (C)} = \frac{I_{output}\left(V_{output} - V_{input}\right)}{f_{sw} * \Delta V * V_{output}} \quad (19)$$

$$\text{Resistor (R)} = \frac{V_{output}}{I_{input}} \quad (20)$$

$$\text{Duty Cycle (D)} = \frac{\left(V_{output} - V_{input}\right)}{V_{output}} \quad (21)$$

Where: $\Delta I = 5\%$ of I_{input}; $\Delta V = 1\%$ of V_{output}

Electric Vehicle (EV) lithium-ion battery behavior was modeled and simulated using MATLAB/Simulink. Parameters applied in the simulation are contained in Table 1.

Table 1: Parameters applied in the simulation for SOC–SOH Fuzzy Logic Modeling

Parameter	Value/Description
Simulation platform	MATLAB/Simulink
Modelling technique	Fuzzy inference system (FIS) and electrochemical modelling
Battery chemistry	Nickel Manganese Cobalt (NMC)
Nominal voltage per cell	3.7 V
Rated capacity	50 Ah
Discharge rates (Coulomb-rate)	1C, 2C, 4C
SOC test levels	20%, 50%, 80%
Ambient temperature scenarios	10°C, 25°C, 45°C
Regenerative braking profiles	City (mild deceleration), Suburban (moderate), Highway (high deceleration, infrequent)
Cycle life reference	500 Equivalent Full Cycles (EFCs)
SOH indicators	Capacity retention and impedance growth
Fuzzy membership functions	Triangular (SOC), Gaussian (C-rate), Trapezoidal (temperature), Sigmoid (SOH output)

Volume 65 | Issue 02 | February 2026
DOI: 10.5281/zenodo.18720371

Inference method	Mamdani-based fuzzy inference
Defuzzification technique	Centroid Method
Optimization technique	Genetic Algorithm (GA) for rule and MF tuning
Validation approach	10-fold cross-validation

The research adopts a simulation-based approach, utilizing MATLAB/Simulink to model and analyze the SOC and SOH of Lithium Ion batteries during regenerative braking. Figure 3 shows the Fuzzy rule formation block diagram of the proposed fuzzy logic control regenerative braking system which focuses on optimizing the amount of energy recovered during braking based on some input parameters such as Braking Power, Speed, and State of Charge (SOC) with a Charging Current as the output. The Fuzzy Logic Controller monitors if the SOC is high which corresponds to the battery being fully charged so that the system can limit the charging current to avoid overcharging. However, if the SOC is low, the system may allow higher charging power to maximize energy recovery. Similarly, Fuzzy Logic Controller monitors the State of Health (SOH) of the battery as being in a good SOH such that it can tolerate higher charging power. A battery with degraded health may require lower charging to minimize stress and prolong its life. Lastly, the fuzzy logic controller monitors the power generated during braking, as higher braking power provides more energy to be potentially recovered, but it needs to be adjusted based on SOC and SOH. Role of Fuzzy Logic Control: Implements intelligent control logic based on linguistic rules to optimize energy recovery and maintain battery health. Figure 3 show the fuzzy logic controller antecedent and consequent evaluation.

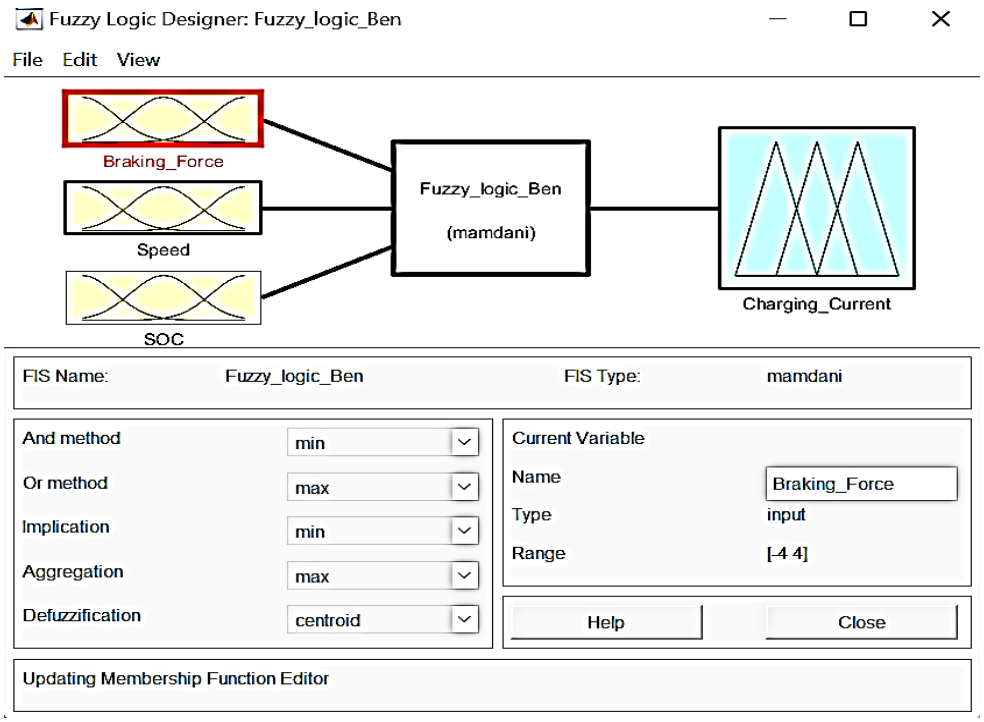

Figure 3: Fuzzy Rule Formation Block Diagram

3.1.1 Formation of Fuzzy Logic Membership Function (Input Variables)

The fuzzy logic controller used for this study consist of three inputs variable namely Breaking Power, Speed and State of Charge (SOC) with three (3) linguistic variable namely; L for low, M for medium, and H for high respectively. All inputs consist of triangular membership function type as shown in Table 2.

Volume 65 | Issue 02 | February 2026
DOI: 10.5281/zenodo.18720371

Table 2: Input Variable Membership Function

Variable	Range	Type	Low	Medium	High
Breaking Power	-4 to 4	Triangular	[-4 -2 0]	[-2 0 2]	[0 2 4]
Speed	0 to 2500	Triangular	[0 500 1000]	[750 1250 1750]	[1500 2000 2500]
State of Charge	0 to 100	Triangular	[59.97 59.98 59.98]	[59.975 59.985 59.995]	[59.99 59.995 60]

The Fuzzy conditions that describe the process of a regenerative braking system (RBS) using fuzzy logic rules for electric vehicle battery optimization. The key steps are:

Initialize input variables: The input variables include Braking Power (Fbrake), Speed (Nm), and Battery State of Charge (SOC). Test for Fuzzy Conditions: The system checks if the following fuzzy conditions are met: check appendix B for fuzzy logic rules.

If the Fuzzy Conditions are met (i.e., Fbrake is High, Nm is High, and SOC is Low), then the Battery Charge mode is Charging as shown in Figure 4.

If the Fuzzy Conditions are met (i.e., Fbrake is Low, Nm is Low, and SOC is High), then the Battery Charge mode is Discharging as shown in Figure 5

If the Fuzzy Conditions are met (i.e., Fbrake is Medium, Nm is High, and SOC is Medium), then the Battery Charge mode is Idle as shown in Figure 6

The purpose of this fuzzy chart is to optimize the regenerative braking performance and ensure efficient energy recovery during the braking process of electric vehicles using fuzzy logic rules, while considering the battery's state of charge and other operating conditions such as the vehicle's speed, braking force, and battery state of charge.

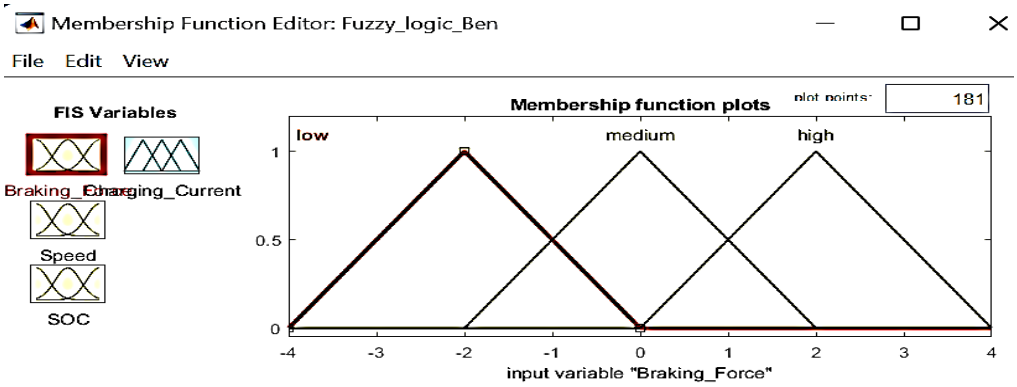

Figure 4: Membership Function Plot for Breaking Power

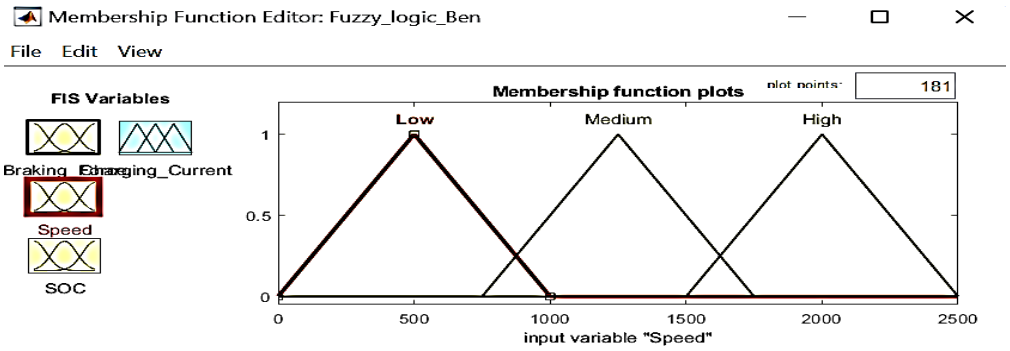

Figure 5: Membership Function Plot for Speed

Volume 65 | Issue 02 | February 2026
DOI: 10.5281/zenodo.18720371

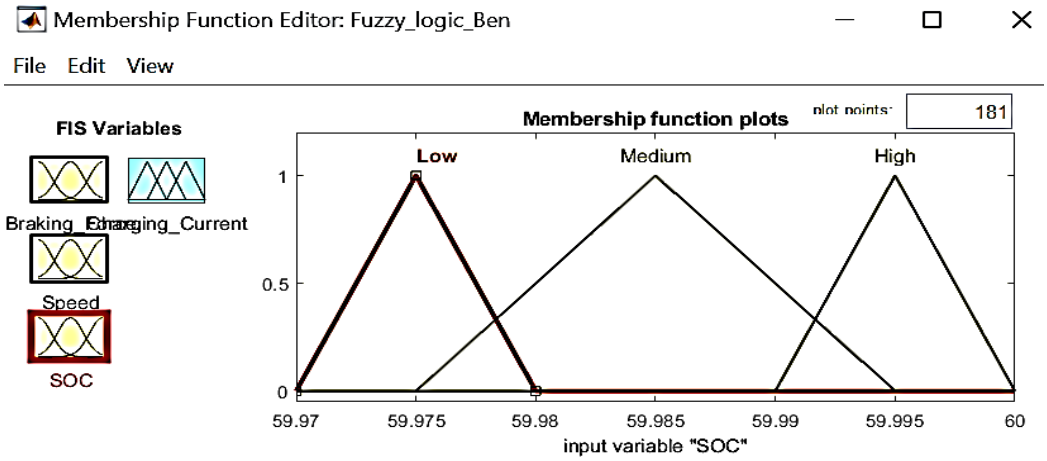

Figure 6: Membership Function Plot for SOC

3.1.2 Output Variables

The fuzzy logic controller used for this study consists of one output variable which is the charging Power as shown in Figure 7. The value ranges from -1 to 1 depending on the unit with three (3) linguistic variables namely; discharge, idle, and charge respectively. All inputs consist of triangle membership function type as shown in Table 3

Table 3: Output Variable Membership Function

Mode	Range	Type	Comment
Charge	[-1 0.75 0]	Triangle	Regenerative braking
Idle	[-0.25 0 0.25]	Triangle	No charge/discharge
Discharge	[0 0.75 1]	Triangle	Acceleration, drawing power

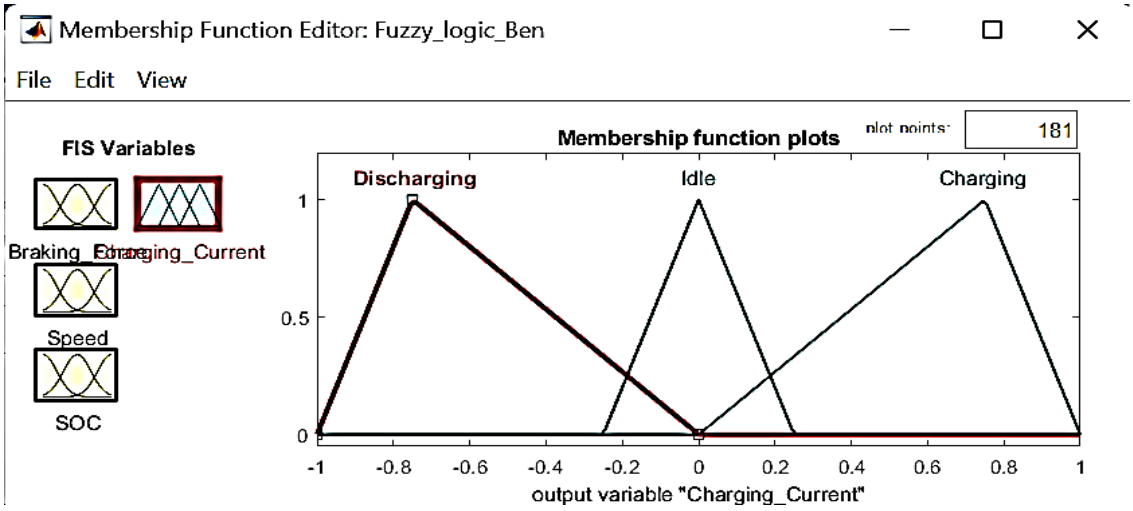

Figure 7: Membership Function Plot for charging power

3.1.3 Formation of Fuzzy Rule

Table 4 shows a summary of the twenty-seven (*27*) fuzzy rule decision matrix for the implementation of the regenerative braking process of the electric vehicle and Figure 8 represents the formation of Fuzzy Rule in MATLAB while Figure 9 represents the Fuzzy Logic Designer for Regenerating Braking. The output rules below indicate whether the system should charge or discharge based on varying levels of Braking Force, Speed, and SOC.

Volume 65 | Issue 02 | February 2026
DOI: 10.5281/zenodo.18720371

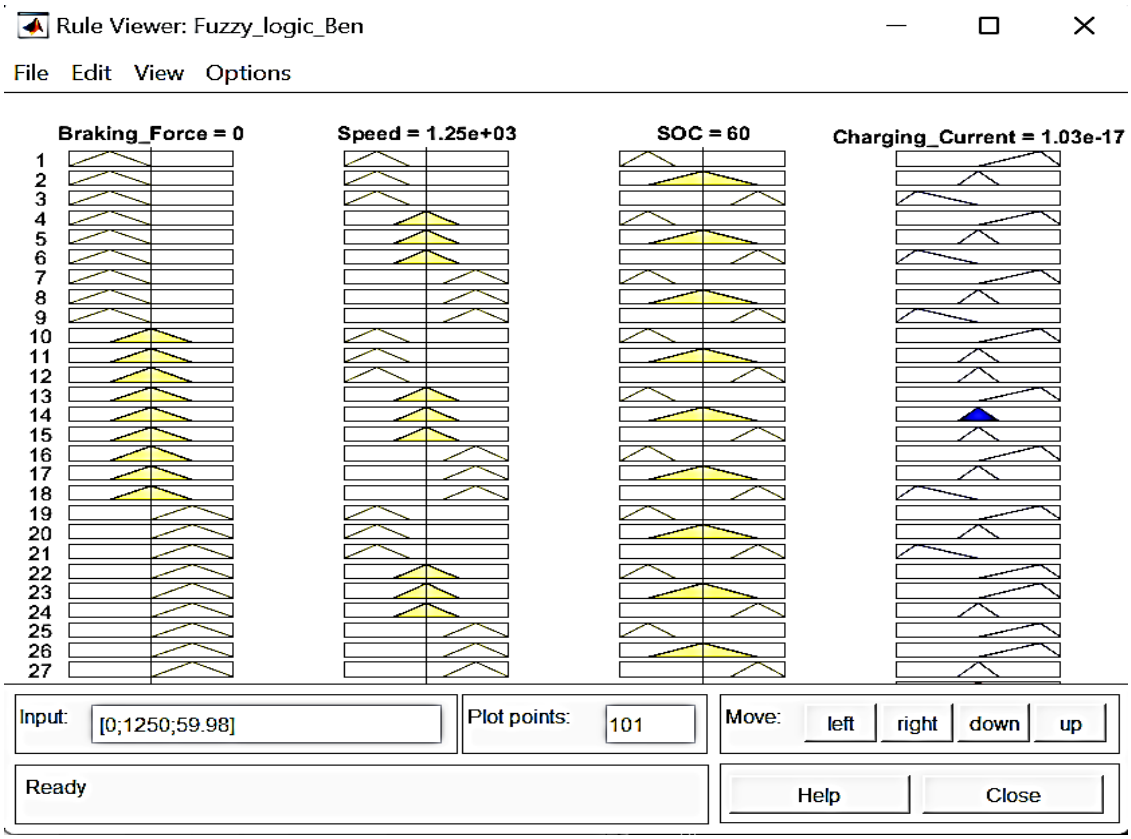

Figure 8: Formation of Fuzzy Rule

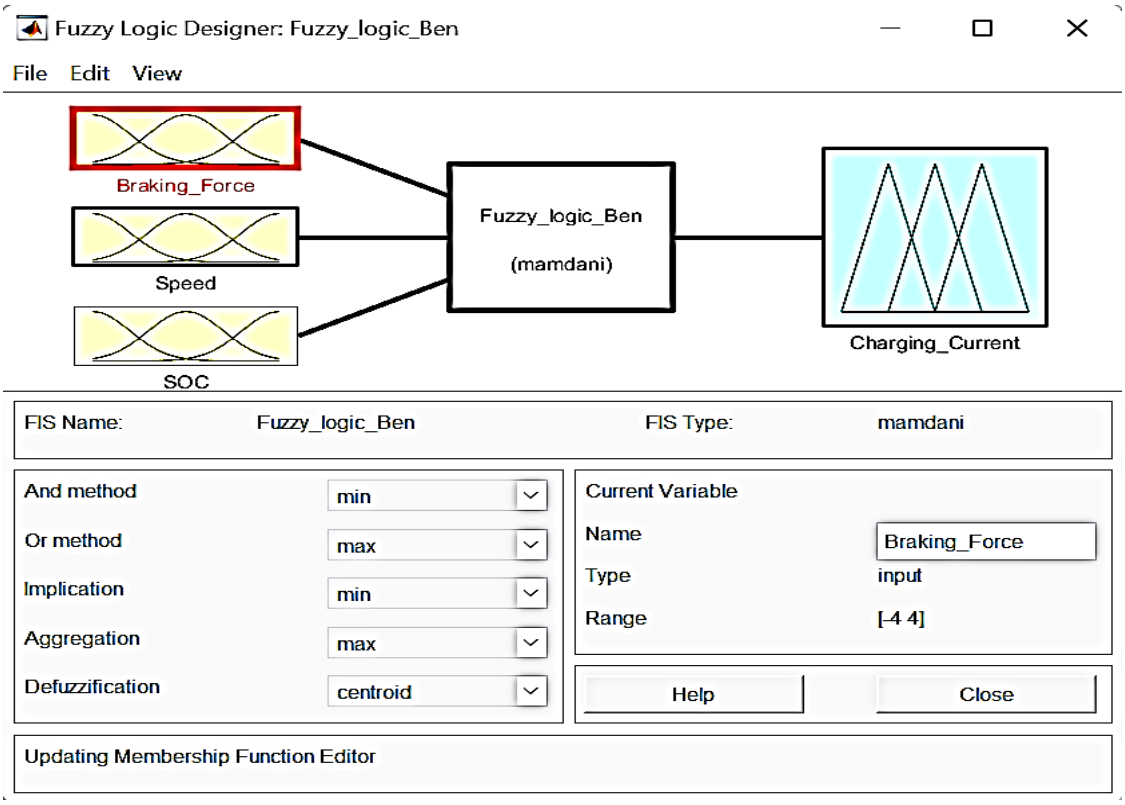

Figure 9: Fuzzy Logic Designer for Regenerating Braking

Volume 65 | Issue 02 | February 2026
DOI: 10.5281/zenodo.18720371

Table 4: Formation of Fuzzy Rule Decision Matrix

SN	Braking Force	Speed	SOC	Charging Current	Explanation
1	Low	Low	Low	Charge (1)	Use all available energy to charge the battery to improve SOC.
2	Low	Low	Medium	Idle (0)	Insufficient energy; avoid stressing the battery with unnecessary charging.
3	Low	Low	High	Discharge (-1)	Overcharging risk; allow battery discharge to power systems instead.
4	Low	Medium	Low	Charge (1)	Moderate energy is available; prioritize SOC improvement.
5	Low	Medium	Medium	Idle (0)	SOC is stable; avoid charging unless essential.
6	Low	Medium	High	Discharge (-1)	Prevent overcharging; use battery power to maintain system operation.
7	Low	High	Low	Charge (1)	High speed generates more energy; fully utilize it for charging.
8	Low	High	Medium	Idle (0)	Balance energy recovery with battery health.
9	Low	High	High	Discharge (-1)	Stop charging and allow discharge to prevent overcharging.
10	Medium	Low	Low	Charge (1)	Energy availability is moderate; charge to improve SOC.
11	Medium	Low	Medium	Idle (0)	Prevent unnecessary cycling as SOC is within an acceptable range.
12	Medium	Low	High	Idle (0)	SOC is already high; avoid further charging.
13	Medium	Medium	Low	Charge (1)	Prioritize charging under moderate speed and braking force conditions.
14	Medium	Medium	Medium	Idle (0)	Balance energy recovery with battery health to avoid overcharging.
15	Medium	Medium	High	Idle (0)	Avoid overcharging by transitioning to idle mode.
16	Medium	High	Low	Charge (1)	Fully utilize the high-speed energy for SOC improvement.
17	Medium	High	Medium	Idle (0)	Moderate SOC; balance energy recovery with stress management.
18	Medium	High	High	Discharge (-1)	Prevent overcharging; allow discharge.
19	High	Low	Low	Charge (1)	Even at low speeds, high braking force provides substantial energy for charging.
20	High	Low	Medium	Idle (0)	Prevent overcharging when SOC is moderate.
21	High	Low	High	Discharge (-1)	Stop charging and allow discharge to reduce SOC.
22	High	Medium	Low	Charge (1)	Substantial energy is available; prioritize SOC recovery.
23	High	Medium	Medium	Charge (1)	SOC improvement is still acceptable under moderate conditions.
24	High	Medium	High	Idle (0)	Prevent overcharging to protect battery health.
25	High	High	Low	Charge (1)	Maximum energy recovery; ensure all energy is used to improve SOC.
26	High	High	Medium	Charge (1)	Energy recovery prioritized while balancing battery stress.
27	High	High	High	Idle (0)	Stop charging and maintain idle mode to avoid overcharging.

Volume 65 | Issue 02 | February 2026
DOI: 10.5281/zenodo.18720371

4. RESULTS AND DISCUSSION

The results of the simulation presented in Figures 10 and 11 showed the effect of the control strategy on the battery SOC and SOH during regenerative braking. Key performance indicators, such as energy recovery efficiency and battery degradation rates were analyzed.

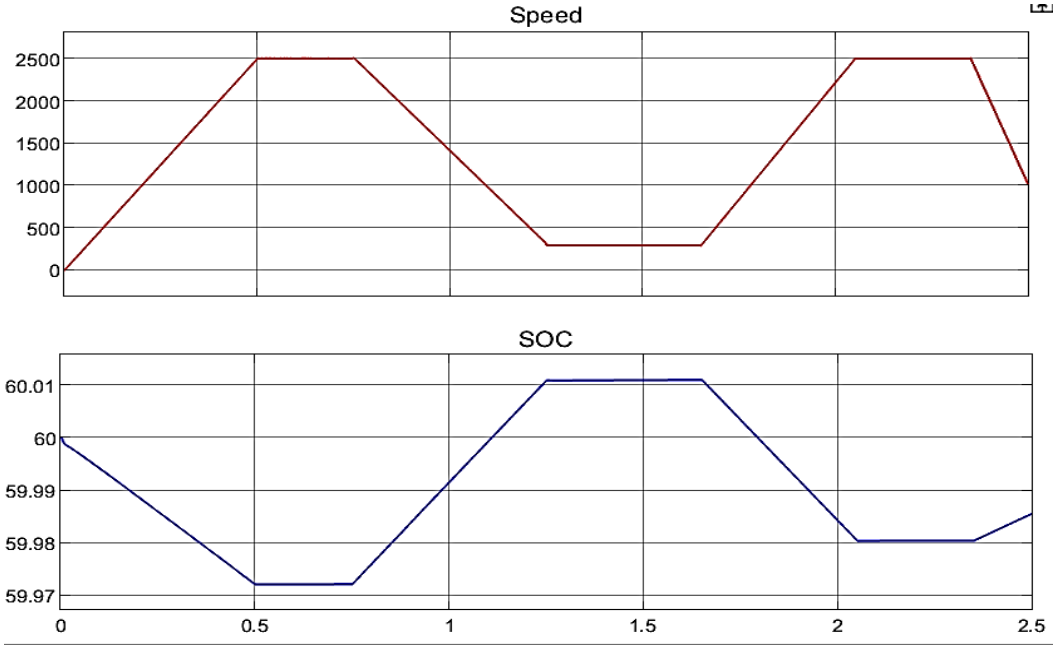

Figure 10: Effect on Battery SOC before and After Regenerative Braking

Figure 10 indicated that at [0.75-1.3] Seconds, when the motor speed is reduced from [2500 to 280] rpm, the state of charge of the battery increased, indicating a charging mode. Similarly, at [2.35-2.5] Seconds, when the motor speed is reduced from 2500rpm to 1000rpm during braking condition, the state of charge of the battery increased, indicating a charging mode. Figure 11 shows the Impact of Regenerative Braking on Battery State of Health

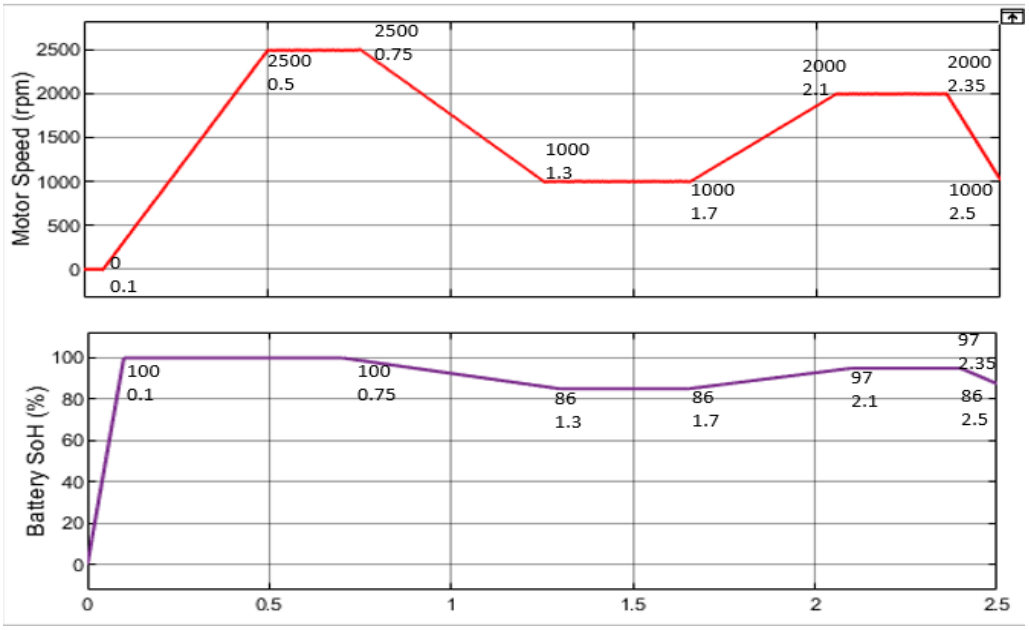

Figure 11: Impact of Regenerative Braking on Battery State of Health

Volume 65 | Issue 02 | February 2026
DOI: 10.5281/zenodo.18720371

It is observed that the State of Health (SOH) of a Lithium Ion battery in electric vehicles (EVs) is a critical indicator of battery performance which decreases with the number of braking events occasioned by reduction in speed. The intensity of braking affects the rate of degradation.

Figure 11 showed that at [0.75-1.3] Seconds when the motor speed reduced from [2500 to 1000] rpm the State of Health (SOH) declined from [100 to 86 to 97 to 86] % as the battery undergoes multiple charge and discharge cycles thereby increasing the internal resistance and generating more heat. Figure 12, shows the impact of regenerative braking on battery current in electric vehicles (EVs).

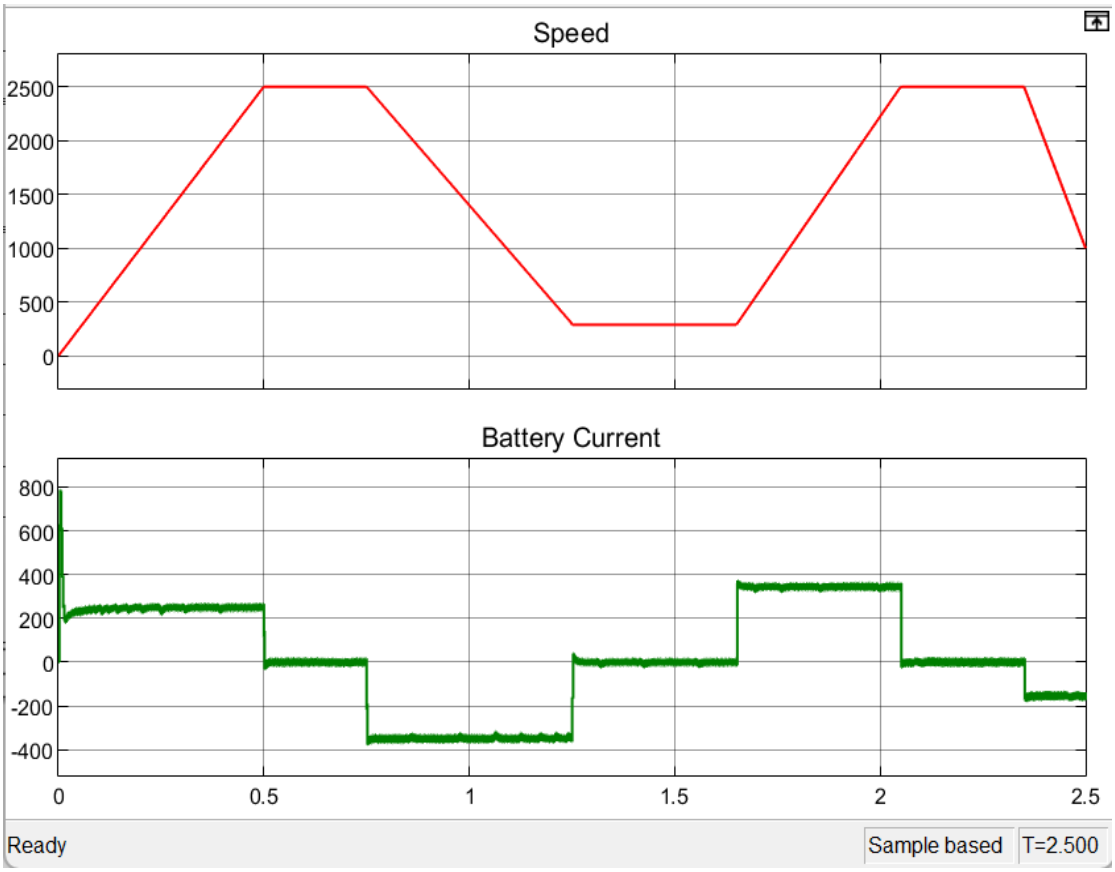

Figure 12: Impact of Braking on Battery Current

During normal operation when the motor is accelerating, the battery discharges to supply the motor. 250A current flows out of the battery which is shown by the positive direction of the current. At [0.5-0.75] Second a uniform speed of 2500 rpm is attained, the battery current drops to 0A and maintains a steady value. At [0.75-1.3] Seconds when regenerative braking was applied, the battery absorbs a charging current as the electrical energy generated by the motor is sent back to the battery which is shown by the negative direction of the current.

The amount of current that flows depends on the intensity of braking, vehicle speed, and motor efficiency. Figure 12 indicates that at [0.75-1.3] Seconds a regenerative braking was applied and motor speed reduced from [2500 to1000] rpm the charging current of the battery was kept at -380A. Similarly, at [2.35 - 2.5] Seconds when a regenerative braking was re-applied the motor speed dropped from [2500 to 1000] rpm while the charging current of the battery was maintained at -150A.

Volume 65 | Issue 02 | February 2026
DOI: 10.5281/zenodo.18720371

The three dimensional plot for the state of charge versus regenerative power versus state of health is shown in the surf plot in Figure 13. The effects of percentage SOC at 20%, 40%, 60%, 80% and 100% on the SOH degradation rates on the EV lithium-ion batteries during regenerative braking conditions was considered.

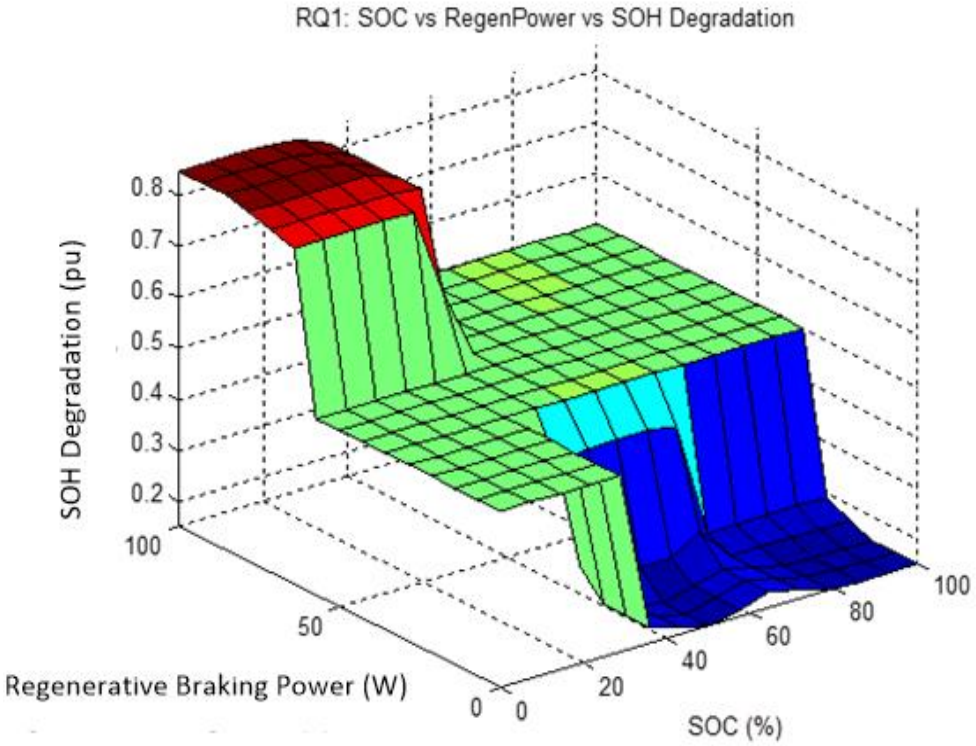

Figure 13: State of Charge versus regenerative braking power versus state of health

In Figure 13, surface plot showed that SOH degradation ranged from 0.30 to 0.85 pu, with a mean value of 0.489 pu and a standard deviation of ±0.221 pu, using impedance growth as the health index. At 20% SOC, degradation peaked above 0.87 pu under highway braking (regenerative current > 80 A), reflecting severe impedance growth due to deep discharge and high braking stress.

In suburban braking between 40% to 60% the same SOC level yielded moderate degradation around 0.63 pu. Similarly, under city braking (<30%), it remained at 0.52 pu. At 50% SOC, the SOH degradation was moderate across all conditions averaging 0.57 pu for highway drive, 0.51 pu for suburban, and 0.45 pu for city drive cycles. At 80% SOC, the state of health degradation remained lowest while maintaining 0.44 pu for highway drive, 0.39 pu for suburban, and 0.31 pu for city drive conditions.

These patterns confirm that SOH deterioration intensifies at lower SOC levels and with severer braking profiles, with the least degradation occurring at 80% SOC under city braking and the highest at 20% SOC under highway braking.

In Figure 14, three dimensional correlations between SOC and SOH under different capacity rates (C) of the battery were presented. 1C, 2C, and 4C discharge rates of lithium-ion batteries were considered.

Volume 65 | Issue 02 | February 2026
DOI: 10.5281/zenodo.18720371

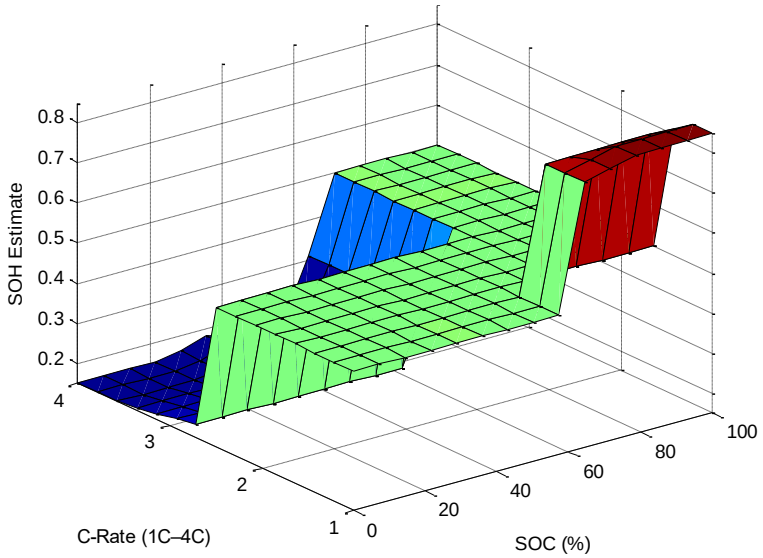

Figure 14: Three dimensional correlations between SOC and SOH under different capacity rate (C)

The three dimensional surface plot showed the SOH estimates ranging from 0.042 to 0.86 pu, with a mean value of 0.493 pu and a standard deviation of ±0.217 pu. At 1C discharge rate, SOH estimates remained high across all SOC levels, averaging 0.69 pu at low SOC and 0.86 pu at high SOC. At 2C discharge rate, degradation intensified slightly with: low SOC value which produced SOH estimates around 0.55 pu. At 4C discharge rate, SOH dropped significantly to 0.32 pu at 20% SOC and 0.51 pu at 50% SOC. Also, at 80% SOC, the SOH estimate remained modest at 0.58 pu. Over 71% of outputs clustered between 0.45–0.63 pu, indicating moderate degradation under realistic conditions. The nonlinear trend confirms that SOH deteriorates rapidly at low SOC under higher discharge rates. Thus, the best SOH performance occurs at 80% SOC with 1C, while the worst-case scenario occurred at 20% SOC with 4C, confirming that both high discharge intensity and low charge depth independently depress battery health. In Figure 15, the three dimensional plot of SOH drift error under varied temperature and regenerative braking is presented. The effectiveness of fuzzy-based nonlinear SOC–SOH estimation in EV-grade lithium-ion batteries operating at varied temperatures of 10°C, 25°C, and 45°C, based on SOH drift error over 100 daily regenerative braking events is well illustrated.

The surface plot showed that the SOH drift error ranging from 0.06 to 0.891 pu was obtained, with a mean value of 0.483 pu and a standard deviation of ±0.226 pu. At 10°C, SOH drift remained low under low-frequency braking (≤ 20 events/day). However, frequent braking (≥ 90 events/day) at the same temperature (10°C) raised drift error to 0.41 pu due to voltage recovery lag. At 25°C, SOH drift remained moderate, rising steadily from 0.31 pu at 30 events/day to 0.46 pu at 100 events/day, reflecting temperature-balanced impedance behavior. At 45°C, thermal acceleration became significant and drift error peaked at 0.86 pu under frequent braking.

Over 69% of outputs clustered between 0.45–0.61 pu, suggesting moderate drift under standard thermal cycling. Therefore, fuzzy modeling revealed that SOH estimation becomes least reliable at high temperatures with frequent braking, and most accurate at moderate temperatures with fewer regenerative events, confirming temperature-braking synergy as a key driver of SOH prediction drift.

Volume 65 | Issue 02 | February 2026
DOI: 10.5281/zenodo.18720371

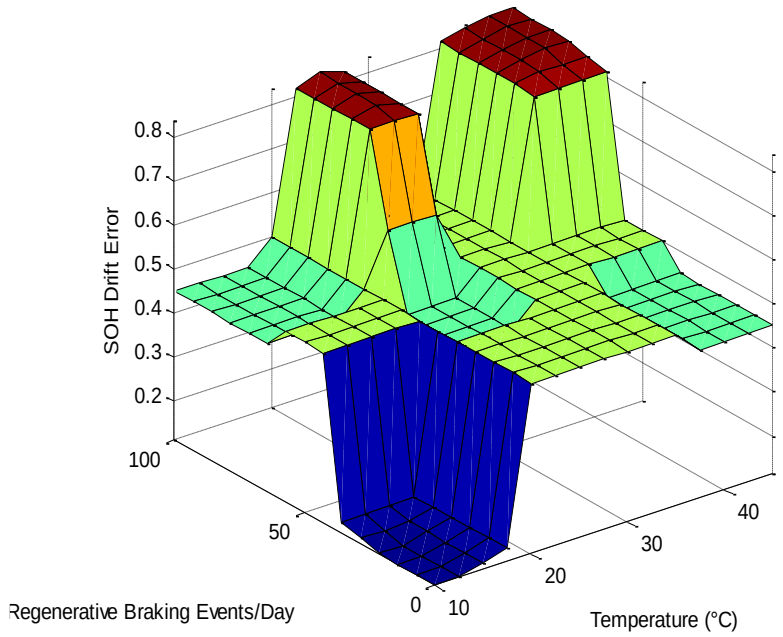

Figure 15: Surface plot of SOH drift error under varied temperature and regenerative braking

A. Result of Fuzzy Logic Battery Optimization Control Strategy

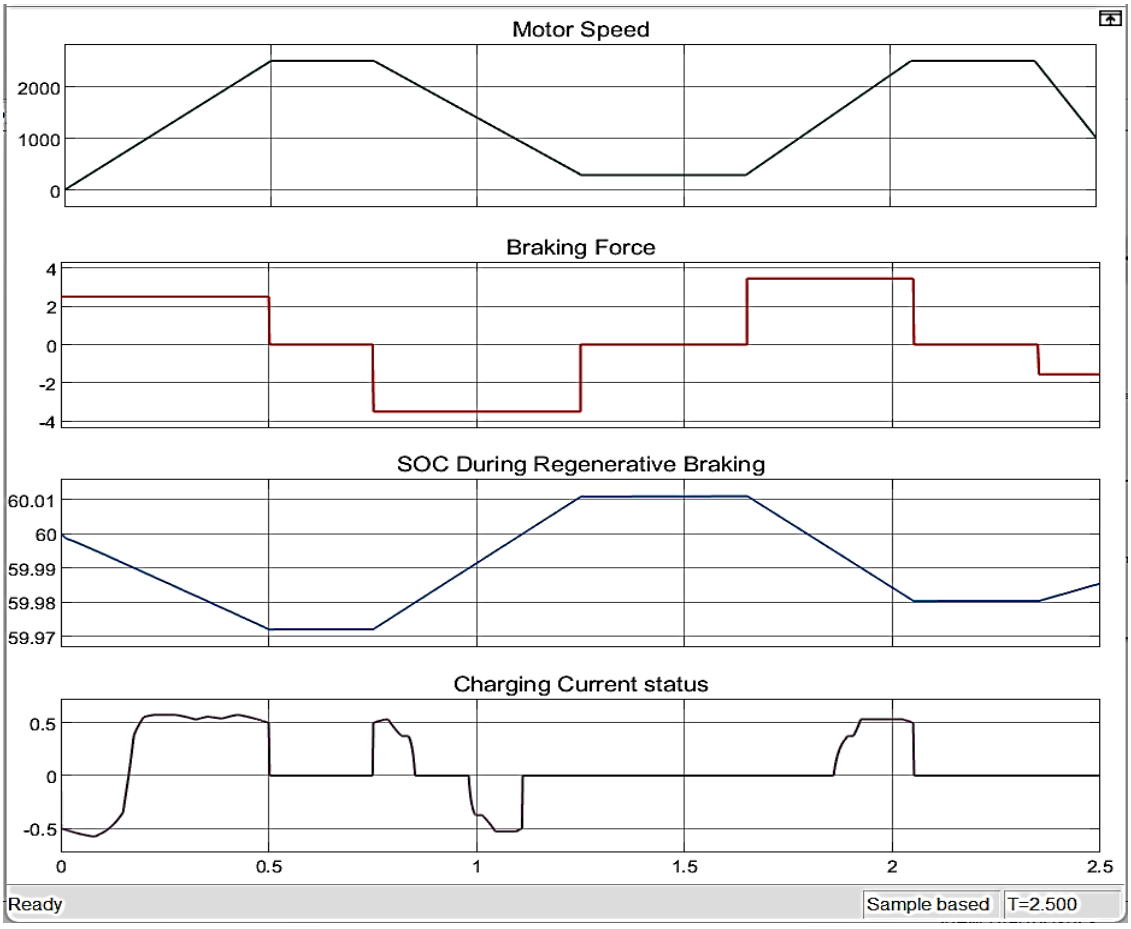

Figure 16: Fuzzy Logic Control for Battery Optimization

Volume 65 | Issue 02 | February 2026
DOI: 10.5281/zenodo.18720371

Figure 16 shows the optimized battery control during charging current stages. Twenty seven (27) fuzzy rules were adopted during this process to determine how much braking energy is used for recharging the battery while ensuring optimal efficiency without stressing the battery or the braking system. Based on the stated rules it shows that If braking Force is high and speed is either medium or low, then the charging current is negative which indicates regenerative braking as shown in Figure 16. Similarly, if braking force is low and speed is either high or medium, then the charging current is Positive which indicates acceleration. The histogram analysis of Fuzzy Logic Controller Inputs and Output is shown in Figure 17. It also showed the comparison of the twenty seven (27) adapted fuzzy rules for battery optimization. The FLC of the EV-drive and its Simulink model is shown in Figure 18. The MATLAB programs are contained in Appendixes A and B.

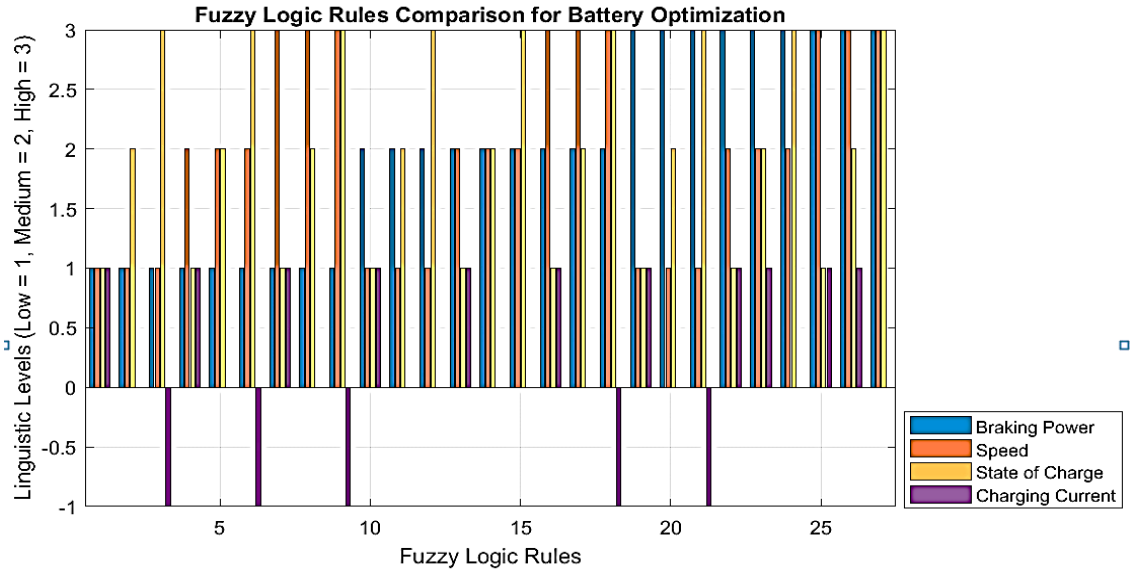

Figure 17: Histogram Analysis of Fuzzy Logic Controller Inputs and Output

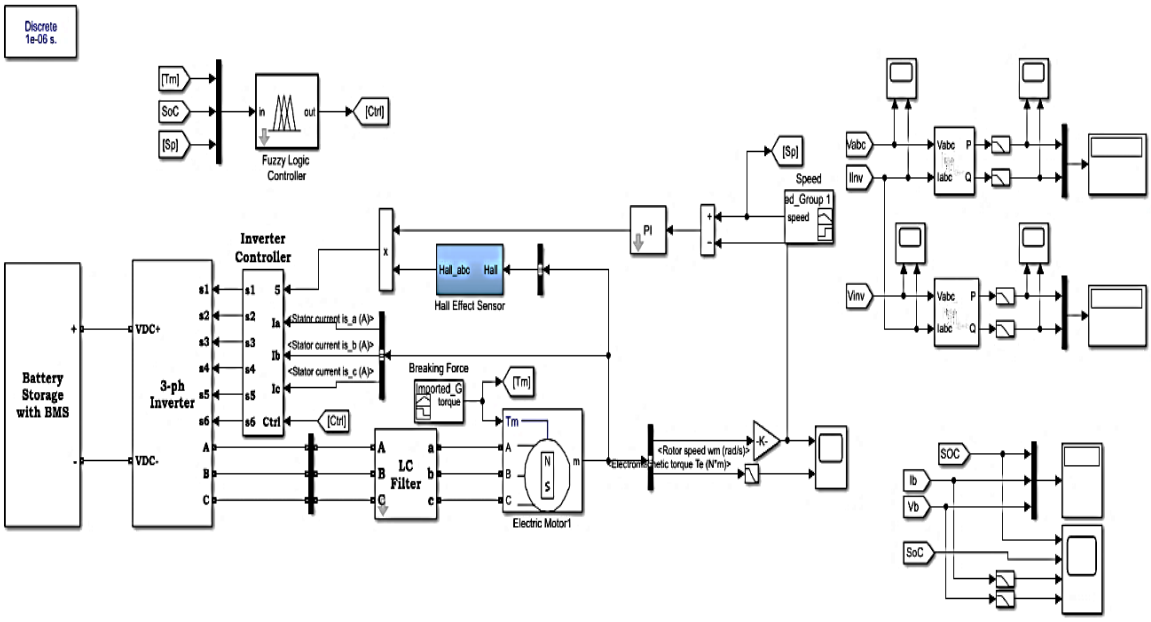

Figure 18: Simulink model of the Fuzzy Logic Controlled Electric Vehicle drive system

Volume 65 | Issue 02 | February 2026
DOI: 10.5281/zenodo.18720371

5. CONCLUSSION AND RECOMMENDATION

A set of fuzzy logic rules have been programmed to monitor and control the electric vehicle battery state of charge and state of health as established in this paper. A simulation was carried out to show the effects of braking force, speed, and SOC of Lithium-ion battery during a regenerative braking system. The simulation results showed that Fuzzy Logic Controller demonstrated superior adaptability and robustness in handling dynamic braking situations for energy recovery enhancement and battery longevity. Simulation results also showed that SOH degradation ranged from 0.30 to 0.85 pu, with a mean value of 0.489 pu and a standard deviation of ±0.221 pu. The steepest degradation occurred at 20% SOC with Capacity rate of four (4C) under a highway braking process. At 80% SOC, the state of health degradation remained lowest while maintaining 0.44 pu for highway drive, 0.39 pu for suburban and 0.31 pu for city drive conditions. Appreciable thermal acceleration was achieved after 45^0 C. A drift error of 0.86 p.u was realized under frequent braking and this maximized energy recovery and minimized battery wear. This research work due to dearth in laboratory facilities was validated through simulations. It is recommended that an experimental prototype will be built in the laboratory in the future work.

REFERENCES

1) S. M., Alavi, A. Khani, and M. Tabrizchi,. Energy recovery optimization in regenerative braking systems for electric vehicles. IEEE Transactions on Vehicular Technology, Vol. 69, no. 4, pp.12-23, 2020.

2) S. Ahmed, and T. Mahmood, Battery SOH optimization in EVs during charging and discharging cycles. International Journal of Energy Research, Vol. 44, no. 9, pp. 67–80, 2020. https://doi.org/10.1002/er.5207

3) M. Amamra, L. Boulon, and Z. Douha, Electric vehicle energy management strategies based on battery state-of-charge feedback: A survey. IEEE Access, Vol.8, pp.644–667, 2020. https://doi.org/10.1109/ACCESS.2020.2981201

4) G..A Asamoah, Nanotechnology-based lithium-ion battery energy storage systems for renewable energy applications. Sustainability, Vol. 16, no. 21, 2024. https://doi.org/10.3390/su16219231

5) J. Bai,, Z. Wang,, S. Liu, C. Zheng, and Y. Xie, A review of data-driven battery health estimation: State of charge, state of health and remaining useful life. Journal of Power Sources, Vol. 487, 229320, 2021. https://doi.org/10.1016/j.jpowsour.2020.229320

6) J.D. Bishop, J. Axsen, and S.M. Skippon, Electric vehicle battery management: Optimization, cost reduction, and lifecycle impacts. Renewable and Sustainable Energy Reviews, Vol. 132, 110087, 2020. https://doi.org/10.1016/j.rser.2020.110087

7) M. Chen, H. Xu, and J. Jiang, A review of Lithium Ion battery safety concerns: The issues, solutions, and future outlook. Journal of Power Sources, Vol. 441, pp. 227-24, 2019. https://doi.org/10.1016/j.jpowsour.2019.03.003

8) Q. Zhou,, L. Shi, and X. Wang, Permanent magnet synchronous machine-based regenerative braking in electric vehicles. IEEE Transactions on Industrial Electronics, Vol.67, no.8, 6734-6742, 2020

Volume 65 | Issue 02 | February 2026
DOI: 10.5281/zenodo.18720371

9) C.O. Omeje, and C.U. Eya. A comparative braking scheme in auto-electric drive systems with permanent magnet synchronous machines. International Journal of Applied Power Engineering Vol. 11, no. 4, pp. 251-263, 2022

10) C.O. Omeje and A.O. Salau, Torque ripples enhancement of a PMBLDC motor propelled through quadratic DC-DC boost converter at varying load, ISA Transaction 143 (2023) 385–397, https://doi.org/10.1016/j.isatra.2023.08.027.

11) C.O. Omeje, A.O. Salau, and C.U. Eya, Dynamics analysis of permanent magnet synchronous motor speed control with enhanced state feedback controller using a linear quadratic regulator. Heliyon 10 (4), 1–15. (2024). https://doi.org/10.1016/j.heliyon.2024.e26018

12) T. Chen, J., Zhao, and Y. Wang, Hybrid SOC Estimation Method for Lithium Ion Batteries in Electric Vehicles. Journal of Energy Storage, Vol. 21, pp.49-58, 2019. https://doi.org/10.1016/j.est.2018.11.002

13) Y. Chen, B. Zhou, and Z. Xu, Energy recovery efficiency of regenerative braking systems in electric vehicles. Energy Reports, Vol. 6, pp. 68-76, 2020.

14) S. Cruz, J. Gama, and R. Silva, Battery management system for electric vehicles: A review. Energy Reports, Vol. 6, pp.207-213, 2020. https://doi.org/10.1016/j.egyr.2019.11.041

15) J. Fan, T. Liu, P. Zhang, and Y. Wang. Regenerative braking energy recovery and SOC optimization in electric vehicles using power electronic converters. Journal of Power Electronics Systems, Vol.29, no. 5, pp.349-360, 2022. https://doi.org/10.1016/j.jpowsys.2022.05.003

16) C. H. Goh, P. Kannan, T. Sundararajan,, & M. Singh, Strategies for reducing carbon emissions through EV battery optimization. Energy Reports, Vol. 8, pp.235-246, 2022. https://doi.org/10.1016/j.egyr.2022.01.024

17) L. Gao,, R..A Douglas, and S. Liu, Power electronics and energy management systems for electric vehicles. IEEE Transactions on Power Electronics, Vol. 33, no. 5, pp.4082-4090, 2018.

18) J.E. Harlow, L. Ma, E.R Logan, and J.R. Dahn. A comprehensive study of the effect of Lithium Ion battery degradation on resale value in electric vehicles. Journal of Electrochemical Energy Conversion and Storage, Vol. 17, no. 2, pp. 71-78, 2020. https://doi.org/10.1115/1.4046250

19) H. He, R. Xiong, J. Fan, and J. Peng. . A practical state of charge estimation method for Lithium Ion batteries based on the extended Kalman filter. Journal of Power Sources, Vol. 255, pp. 175-182, 2020. https://doi.org/10.1016/j.jpowsour.2013.12.037

20) B.H Kang, H.S. Kim, and K. Lee, A study on the thermal management of power electronics in electric vehicles. Energies, Vol. 14, no. 15, pp.47-72, 2021. https://doi.org/10.3390/en14154727

21) M. Liu., J. Zhao, and Q. Wei, . Energy management in regenerative braking of electric vehicles: A control algorithm and system model. IEEE Transactions on Vehicular Technology, Vol.70, no.6, pp.5390-5400, 2021.. https://doi.org/10.1109/TVT.2021.3074499

Volume 65 | Issue 02 | February 2026
DOI: 10.5281/zenodo.18720371

22) L. Luo, X. Liang, and X. Zhao. The impact of temperature on Lithium Ion battery performance: A comprehensive review. Journal of Power Electronics and Applications, Vol.19, no. 5, pp.157–171, 2021. https://doi.org/10.1007/s11708-021-0736-3

23) A. Singh, J. Patel, and J. Thomas. Role of battery management systems in extending lithium-ion battery lifespan in EVs. Renewable Energy Research and Applications, Vol.19, no.4, pp. 278–289, 2023. https://doi.org/10.1016/j.rera.2023.101478

24) X. Wang, Z. Zhou, and F. Xu, Advanced energy management strategies for Lithium Ion batteries in electric vehicles. Energy Reports, Vol. 8, no.1, pp. 911–921, 2022. https://doi.org/10.1016/j.egyr.2022.03.057

25) H. Yang, X. Wang, Y. and Zheng, Optimizing SOC estimation and thermal management of Lithium Ion batteries in electric vehicles. International Journal of Energy Research, Vol.46, no.11, pp.1457-1470, 2022. https://doi.org/10.1002/er.7585

26) E. Omorogiuwa, and C. N. Eze, Optimization of SOC, temperature, and SOH of lithium-ion batteries in electric vehicles using MATLAB/Simscape. Journal of Energy Technology, Vol.15, no.3, pp. 145-160, 2020. https://doi.org/10.1016/j.energytech.2020.04.001.

27) X. Yang, Z. Liu, and P. Chen, Real-time optimization of SOC and SOH in electric vehicle regenerative braking. International Journal of Power Electronics, Vol. 39, no.1, pp.103-118, 2024. https://doi.org/10.1016/j.ijpe.2024.01.001

28) H. Zhang, and Z. Wang, Battery management system design and optimization for electric vehicle applications: A case study. IEEE Transactions on Power Electronics, Vol.36, no.4, pp.3678-3689, 2021. https://doi.org/10.1109/TPEL.2021.3051899

29) X. Zhang, Y. Gao, and M. Ehsani. Model-based optimization of regenerative braking system in electric vehicles. IEEE Transactions on Vehicular Technology, Vol.69, no.8, pp.7830-7842, 2020.

30) J.G. Hayes and G.A. Goodarzi, Electric Power Train. John Wiley ltd, U.S.A 2018.

APPENDIX A

[System]

Name='Regenerative_Braking'

Type='mamdani'

Version=2.0

NumInputs=3

NumOutputs=1

NumRules=12

AndMethod='min'

OrMethod='max'

ImpMethod='min'

AggMethod='max'

DefuzzMethod='centroid'

Volume 65 | Issue 02 | February 2026
DOI: 10.5281/zenodo.18720371

```
[Input1]
Name='Breaking_Force'
Range=[-4 4]
NumMFs=3
MF1='Low':'trimf',[-4 -2 0]
MF2='Medium':'trimf',[-2 0 2]
MF3='High':'trimf',[0 2 4]
[Input2]
Name='Speed'
Range=[0 2500]
NumMFs=3
MF1='Low':'trimf',[0 500 1000]
MF2='Medium':'trimf',[750 1250 1750]
MF3='High':'trimf',[1500 2000 2500]
[Input3]
Name='Battery_SoC'
Range=[0 100]
NumMFs=3
MF1='Low':'trimf',[59.97 59.975 59.98]
MF2='Medium':'trimf',[59.975 59.985 59.995]
MF3='High':'trimf',[59.99 59.995 60]
[Output1]
Name='Charging_Current'
Range=[-20 20]
NumMFs=3
MF1='Charge':'trimf',[-1 -0.75 0]
MF2='Idle':'trimf',[-0.25 0 0.25]
MF3='Discharge':'trimf',[0 0.75 1]
[Rules]
rules = [
    "If BrakingForce is Low and Speed is Low and SOC is Low then ChargingCurrent is Charge";
    "If BrakingForce is Low and Speed is Low and SOC is Medium then ChargingCurrent is Idle";
    "If BrakingForce is Low and Speed is Low and SOC is High then ChargingCurrent is Discharge";
    "If BrakingForce is Low and Speed is Medium and SOC is Low then ChargingCurrent is Charge";
    "If BrakingForce is Low and Speed is Medium and SOC is Medium then ChargingCurrent is Idle";
```

Volume 65 | Issue 02 | February 2026
DOI: 10.5281/zenodo.18720371

```
    "If BrakingForce is Low and Speed is Medium and SOC is High then ChargingCurrent is Discharge";
    "If BrakingForce is Low and Speed is High and SOC is Low then ChargingCurrent is Charge";
    "If BrakingForce is Low and Speed is High and SOC is Medium then ChargingCurrent is Idle";
    "If BrakingForce is Low and Speed is High and SOC is High then ChargingCurrent is Discharge";
    "If BrakingForce is Medium and Speed is Low and SOC is Low then ChargingCurrent is Charge";
    "If BrakingForce is Medium and Speed is Low and SOC is Medium then ChargingCurrent is Idle";
    "If BrakingForce is Medium and Speed is Low and SOC is High then ChargingCurrent is Idle";
    "If BrakingForce is Medium and Speed is Medium and SOC is Low then ChargingCurrent is Charge";
    "If BrakingForce is Medium and Speed is Medium and SOC is Medium then ChargingCurrent is
Idle";
    "If BrakingForce is Medium and Speed is Medium and SOC is High then ChargingCurrent is Idle";
    "If BrakingForce is Medium and Speed is High and SOC is Low then ChargingCurrent is Charge";
    "If BrakingForce is Medium and Speed is High and SOC is Medium then ChargingCurrent is Idle";
    "If BrakingForce is Medium and Speed is High and SOC is High then ChargingCurrent is Discharge";
    "If BrakingForce is High and Speed is Low and SOC is Low then ChargingCurrent is Charge";
    "If BrakingForce is High and Speed is Low and SOC is Medium then ChargingCurrent is Idle";
    "If BrakingForce is High and Speed is Low and SOC is High then ChargingCurrent is Discharge";
    "If BrakingForce is High and Speed is Medium and SOC is Low then ChargingCurrent is Charge";
    "If BrakingForce is High and Speed is Medium and SOC is Medium then ChargingCurrent is
Charge";
    "If BrakingForce is High and Speed is Medium and SOC is High then ChargingCurrent is Idle";
    "If BrakingForce is High and Speed is High and SOC is Low then ChargingCurrent is Charge";
    "If BrakingForce is High and Speed is High and SOC is Medium then ChargingCurrent is Charge";
    "If BrakingForce is High and Speed is High and SOC is High then ChargingCurrent is Idle";
];
fis = addRule(fis, rules);
```

APPENDIX B

```
% Define numeric representations for each linguistic level for plotting
 % Breaking Force (Low, Medium, High)
breaking_power_levels = [1, 1, 1, 1, 1, 1, 1, 1, 1, 2, 2, 2, 2, 2, 2, 2, 2, 2, 3, 3, 3, 3, 3, 3, 3, 3, 3];
% High = 3, Medium = 2, Low = 1
 % Speed (Low, Medium, High)
speed_levels = [1, 1, 1, 2, 2, 2, 3, 3, 3, 1, 1, 1, 2, 2, 2, 3, 3, 3, 1, 1, 1, 2, 2, 2, 3, 3, 3];
% High = 3, Medium = 2, Low = 1
 % State of Charge (SoC) (Low, Medium, High)
soc_levels = [1, 2, 3, 1, 2, 3, 1, 2, 3, 1, 2, 3, 1, 2, 3, 1, 2, 3, 1, 2, 3, 1, 2, 3, 1, 2, 3];
```

Volume 65 | Issue 02 | February 2026
DOI: 10.5281/zenodo.18720371

```
% Low = 1, Medium = 2, High = 3
 % Charging Current (Discharge, Charge, Idle)
charging_current_levels = [1, 0, -1, 1, 0, -1, 1, 0, -1, 1, 0, 0, 1, 0, 0, 1, 0, -1, 1, 0, -1, 1, 1, 0, 1, 1, 0];
% Discharge = -1, Charge = 1, Idle = 0
 % Define rule names for the 27 fuzzy rules
input_sets = {'Rule 1', 'Rule 2', 'Rule 3', 'Rule 4', 'Rule 5', 'Rule 6', 'Rule 7', 'Rule 8', 'Rule 9', 'Rule 10',
'Rule 11', 'Rule 12', 'Rule 13', 'Rule 14', 'Rule 15', 'Rule 16', 'Rule 17', 'Rule 18', 'Rule 19', 'Rule 20',
'Rule 21', 'Rule 22', 'Rule 23', 'Rule 24', 'Rule 25', 'Rule 26', 'Rule 27'};
 % Combine input and output variables into a matrix
data_matrix = [breaking_power_levels; speed_levels; soc_levels; charging_current_levels]';
 % Display the data to verify input
disp('Fuzzy Logic Rule Matrix:');
disp(data_matrix);

% Plot the bar chart for the rules
figure;
bar(data_matrix, 'grouped'); % Grouped bar chart for comparison
set(gca, 'xticklabel', input_sets); % Label each rule
xlabel('Fuzzy Logic Rules');
ylabel('Linguistic Levels (Low = 1, Medium = 2, High = 3)');
legend('Braking Power', 'Speed', 'State of Charge', 'Charging Current');
title('Fuzzy Logic Rules Comparison for Battery Optimization');
grid on;
 % Optional: Adjust bar colors for clarity
colormap(jet); % Customize colormap if desired
```